


Modulation of Fluorophore Environment in Host Membranes of Varying Charge

View metadata, citation and similar papers at core.ac.uk

brought to you by  CORE

provided by Publications of the IAS Fellows

Devaki A. Kelkar,¹ Anuradha Ghosh,¹ and Amitabha Chattopadhyay^{1,2}

Received April 18, 2003; revised August 1, 2003; accepted August 3, 2003

The net electrical charge of the biological membrane represents an important parameter in the organization, dynamics and function of the membrane. In this paper, we have characterized the change in the microenvironment experienced by a membrane-bound fluorescent probe when the charge of the phospholipids constituting the host membrane is changed from zwitterionic to cationic with minimal change in the chemical structure of the host lipid. In particular, we have explored the difference in the microenvironment experienced by the fluorescent probe 2-(9-anthroyloxy)stearic acid (2-AS) in model membranes of zwitterionic 1-palmitoyl-2-oleoyl-*sn*-glycero-3-phosphocholine (POPC) and cationic 1-palmitoyl-2-oleoyl-*sn*-glycero-3-ethylphosphocholine (EPOPC) which are otherwise chemically similar, using the wavelength-selective fluorescence approach and other fluorescence parameters. Our results show that the microenvironment experienced by a membrane probe such as 2-AS is different in POPC and EPOPC membranes, as reported by red edge excitation shift (REES) and other fluorescence parameters. The difference in environment encountered by the probe in the two cases could possibly be due to variation in hydration in the two membranes owing to different charges.

KEY WORDS: Membrane charge; wavelength-selective fluorescence; red edge excitation shift; cationic lipid.

INTRODUCTION

A direct consequence of organized molecular assemblies such as membranes is the restriction imposed on the dynamics and mobility of the constituent structural units. We have previously shown that the microenvironment of molecules bound to such organized assemblies can be conveniently monitored using wavelength-selective fluorescence as a novel tool [1]. Wavelength-selective fluorescence comprises a set of approaches based on the red edge effect in fluorescence spectroscopy which can be used to directly monitor the environment and dynamics around a fluorophore in a complex biological system [2–4]. A shift in the wavelength of maximum fluorescence emission toward higher wavelengths, caused by a shift in the

excitation wavelength toward the red edge of the absorption band, is termed the red edge excitation shift (REES). This effect is mostly observed with polar fluorophores in motionally restricted media such as very viscous solutions or condensed phases where the dipolar relaxation (reorientation) time for the solvent shell around an excited state fluorophore is comparable to or longer than its fluorescence lifetime [2–6]. Utilizing this approach, it becomes possible to probe the mobility parameters of the environment itself (which is represented by the relaxing solvent molecules) using the fluorophore merely as a reporter group. Further, since the ubiquitous solvent for biological systems is water, the information obtained in such cases will come from the otherwise “optically silent” water molecules. This makes REES and related techniques extremely useful in biology since hydration plays a crucial modulatory role in a large number of important cellular events [7,8] such as lipid-protein interactions [9] and ion transport [10–12]. We have earlier shown that REES and related techniques (wavelength-selective fluorescence

¹ Centre for Cellular and Molecular Biology, Uppal Road, Hyderabad 500007, India.

² To whom correspondence should be addressed. E-mail: amit@ccmb.res.in

approach) serve as a powerful tool to monitor organization and dynamics of membrane-bound probes and peptides [1,13–17].

The net electrical charge of the biological membrane represents an important parameter in the organization, dynamics and function of the membrane. The electrostatic interfacial potential generated at the membrane-solution interface due to the membrane charge plays a crucial role in a variety of membrane-associated phenomena including activity of membrane proteins and receptors, ion binding and transport, ligand recognition, and interaction with other membranes [18]. In this paper, we have characterized the change in organization and dynamics of a membrane-bound fluorescent probe when the charge of the phospholipids constituting the host membrane is changed from zwitterionic to cationic with minimal change in the chemical structure of the host lipid. In particular, we have explored the difference in the microenvironment experienced by the fluorescent probe 2-(9-anthroyloxy)stearic acid (2-AS) in model membranes of zwitterionic 1-palmitoyl-2-oleoyl-*sn*-glycero-3-phosphocholine (POPC) and cationic 1-palmitoyl-2-oleoyl-*sn*-glycero-3-ethylphosphocholine (EPOPC) which are otherwise chemically similar (see

Fig. 1), using the wavelength-selective fluorescence approach and other fluorescence parameters. Our results show that even a subtle change in lipid chemistry resulting in a change in the charge type could give rise to considerable difference in the microenvironment experienced by a membrane embedded molecule as reported by various fluorescence parameters.

EXPERIMENTAL

Materials

POPC and EPOPC were obtained from Avanti Polar Lipids (Alabaster, AL). Dimyristoyl-*sn*-glycero-3-phosphocholine (DMPC) was obtained from Sigma (St. Louis, MO). 2-AS was from Molecular Probes (Eugene, OR). Lipids were checked for purity by thin-layer chromatography on silica gel precoated plates (Sigma) in chloroform/methanol/conc. ammonia (65:25:4, v/v/v) [19] and were found to give only one spot in all cases with a phosphate-sensitive spray and on subsequent charring [20]. The concentration of lipids was determined by phosphate assay subsequent to total digestion by perchloric acid [21]. DMPC was used as an internal standard to

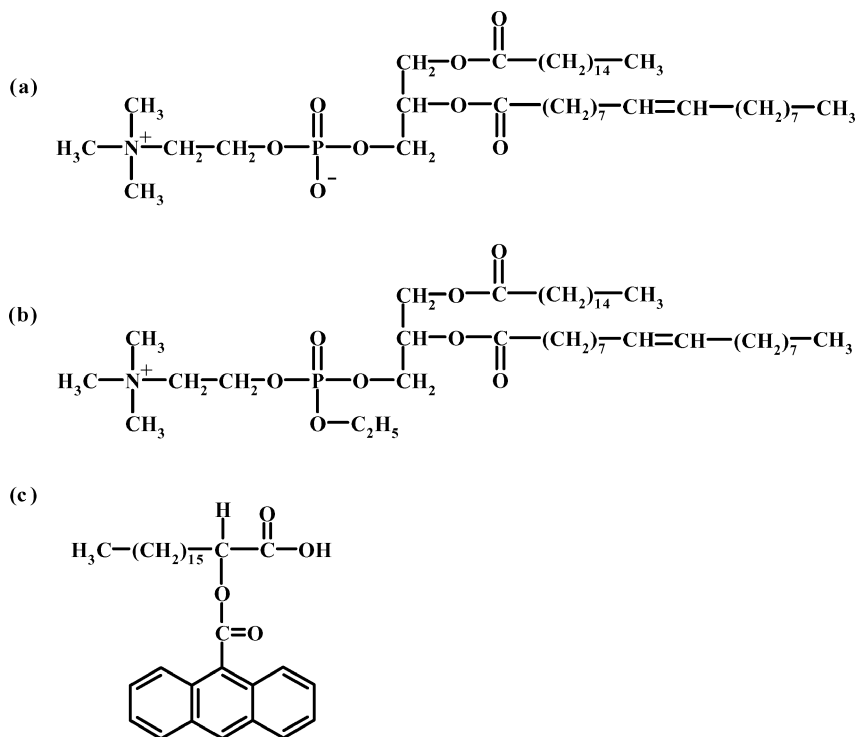


Fig. 1. Chemical structures of (a) POPC, (b) EPOPC, and (c) 2-AS. Notice that while POPC is zwitterionic, EPOPC is cationic. The structure of 2-AS shown is the protonated form which is the predominant form under experimental conditions (pH 5). See text for other details.

assess lipid digestion. Concentrations of stock solutions of 2-AS in methanol were estimated using the molar extinction coefficient (ϵ) of $8,000 \text{ M}^{-1} \text{ cm}^{-1}$ at 361 nm [22]. All other chemicals used were of the highest purity available. Solvents used were of spectroscopic grade. Water was purified through a Millipore (Bedford, MA) Milli-Q system and used throughout.

Methods

All experiments were done using large unilamellar vesicles (LUVs) of 100 nm diameter containing $1 \text{ mol}\%$ 2-AS. In general, 200 nmol (1280 nmol for time-resolved fluorescence measurements) of lipid (POPC or EPOPC) in methanol/chloroform was mixed with 2 nmol (12.8 nmol for time-resolved fluorescence measurements) of 2-AS in methanol. The sample was mixed well and dried under a stream of nitrogen while being warmed gently ($\sim 35^\circ \text{C}$). After further drying under a high vacuum for at least 3 hr , 1.5 mL of 10 mM sodium acetate, 150 mM sodium chloride, $\text{pH } 5.0$ buffer was added, and the sample was vortexed for three minutes to disperse the lipid and form homogeneous multilamellar vesicles. LUVs of 100 nm diameter were prepared by the extrusion technique using an Avestin Liposofast Extruder (Ottawa, Ontario, Canada) as previously described [23]. Briefly, the multilamellar vesicles were freeze-thawed five times using liquid nitrogen to ensure solute equilibration between trapped and bulk solutions, and then extruded through polycarbonate filters (pore diameter of 100 nm) mounted in the extruder fitted with Hamilton syringes (Hamilton Company, Reno, NV). The samples were subjected to 11 passes through the polycarbonate filter to give the final LUV suspension. Samples were kept overnight in the dark at room temperature for equilibration before making measurements.

Steady State Fluorescence Measurements

Steady state fluorescence measurements were performed with a Hitachi F-4010 spectrofluorometer using 1 cm path length quartz cuvettes. Excitation and emission slits with a nominal bandpass of 5 nm were used for all measurements. Background intensities of samples in which the fluorophore 2-AS was omitted were negligible in most cases and were subtracted from each sample spectrum to cancel out any contribution due to the solvent Raman peak and other scattering artifacts. The spectral shifts obtained with different sets of samples were identical in most cases. In other cases, the values were within $\pm 1 \text{ nm}$ of the ones reported. Fluorescence polarization measurements were performed using a Hitachi polariza-

tion accessory. Polarization values were calculated from the equation [24]:

$$P = \frac{I_{VV} - GI_{VH}}{I_{VV} + GI_{VH}} \quad (1)$$

where I_{VV} and I_{VH} are the measured fluorescence intensities (after appropriate background subtraction) with the excitation polarizer vertically oriented and emission polarizer vertically and horizontally oriented, respectively. G is the grating correction factor and is equal to I_{HV}/I_{HH} . All experiments were done with multiple sets of samples and average values of polarization are shown in the figures.

Time-Resolved Fluorescence Measurements

Fluorescence lifetimes were calculated from time-resolved fluorescence intensity decays using a Photon Technology International (London, Western Ontario, Canada) LS-100 luminescence spectrophotometer in the time-correlated single photon counting mode. This machine uses a thyratron-gated nanosecond flash lamp filled with nitrogen as the plasma gas (16 ± 1 inches of mercury vacuum) and is run at $17\text{--}18 \text{ kHz}$. Lamp profiles were measured at the excitation wavelength using Ludox (colloidal silica) as the scatterer. To optimize the signal to noise ratio, 5000 photon counts were collected in the peak channel. The excitation wavelength used was 365 nm . Emission wavelength was set at 460 nm . All experiments were performed using excitation and emission slits with a nominal bandpass of 3 nm or less. The sample and the scatterer were alternated after every 10% acquisition to ensure compensation for shape and timing drifts occurring during the period of data collection. This arrangement also prevents any prolonged exposure of the sample to the excitation beam thereby avoiding any possible photodamage during data acquisition. The data stored in a multichannel analyzer was routinely transferred to an IBM PC for analysis. Intensity decay curves so obtained were fitted as a sum of exponential terms:

$$F(t) = \sum_i \alpha_i \exp(-t/\tau_i) \quad (2)$$

where α_i is a preexponential factor representing the fractional contribution to the time-resolved decay of the component with a lifetime τ_i . The decay parameters were recovered using a nonlinear least squares iterative fitting procedure based on the Marquardt algorithm [25]. The program also includes statistical and plotting subroutine packages [26]. The goodness of the fit of a given set of observed data and the chosen function was evaluated by the reduced χ^2 ratio, the weighted residuals [27], and the autocorrelation function of the weighted residuals [28]. A

fit was considered acceptable when plots of the weighted residuals and the autocorrelation function showed random deviation about zero with a minimum χ^2 value not more than 1.2. Mean (average) lifetimes $\langle\tau\rangle$ for biexponential decays of fluorescence were calculated from the decay times and preexponential factors using the following equation [29]:

$$\langle\tau\rangle = \frac{\alpha_1\tau_1^2 + \alpha_2\tau_2^2}{\alpha_1\tau_1 + \alpha_2\tau_2} \quad (3)$$

RESULTS

Fig. 1 (a and b) shows the chemical structures of POPC and EPOPC, the two phospholipids used in this study. Their structures are identical except that EPOPC has an ethyl group attached to one of the phosphate oxygen atoms through an ester bond. This neutralizes the negative charge resulting in the cationic nature of EPOPC due to the remaining positive charge on the choline headgroup. Cationic lipids such as EPOPC have previously been used as efficient transfection agents [30]. An interesting feature of EPOPC is that it is chemically similar to naturally occurring lipids though it is cationic in nature. This is in contrast to the cationic lipids such as 1,2-dioleoyloxy-3-(trimethylammonio)propane (DOTAP) which represent an earlier generation of cationic lipids and are still extensively used for delivering DNA to eukaryotic cells [31].

Fig. 1(c) shows the chemical structure of 2-AS, the fluorescent probe used. Fatty acids labeled with spectroscopic reporter groups have proved to be useful membrane probes [16]. The anthroyloxy fatty acids such as 2-AS in which an anthracene group is attached by an ester linkage to an alkyl chain have been extensively used as fluorescent probes in membranes [16,32-35]. Depth analysis using the parallax method [36] has previously shown that the anthroyloxy group in 2-AS in its protonated form is localized at the membrane interface at a depth of 15.8 Å from the center of the membrane bilayer [37]. Importantly, 2-AS is ideally suited for wavelength-selective fluorescence studies since it exhibits a large change in dipole moment (4.5 D) upon excitation [38], an important criterion for displaying REES [2,4].

Our goal was to explore the change in organization and dynamics of a membrane-bound fluorescent probe when the charge of the phospholipids constituting the host membrane is changed from zwitterionic to cationic. Ideally, this should be accompanied by minimal change in the chemical structure of the host lipid, a requirement that is fulfilled by POPC and EPOPC since they differ only by an ethyl group. Another important criterion was that the

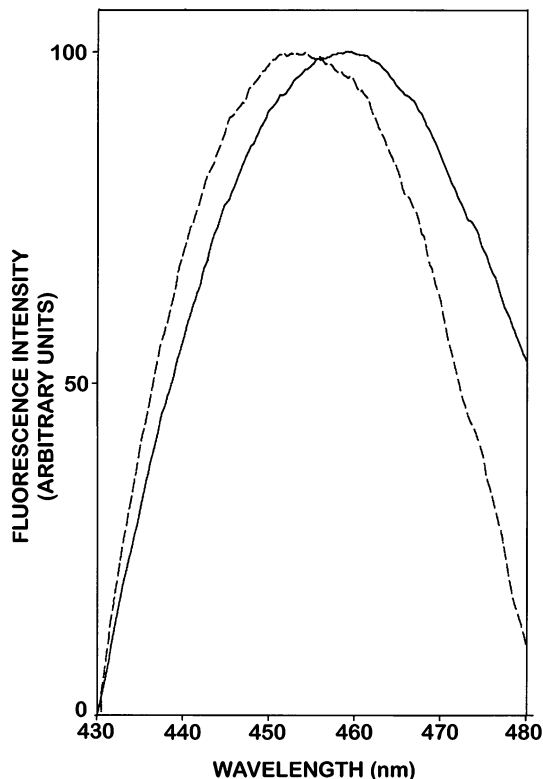


Fig. 2. Fluorescence emission spectra of 2-AS in LUVs of POPC (—) and EPOPC (---). The concentration of lipid was 0.13 mM and probe to lipid ratio was 1:100 (mol/mol). The spectra are intensity-normalized to the emission maximum. The excitation wavelength was 365 nm in both cases. See Experimental for other details.

probe itself should be electrically neutral under the conditions of the experiment to avoid any artifacts due to charge interactions. In order to meet this criterion, all experiments were done at pH 5. Since the pK_a of membrane-bound 2-AS is ~ 7 [39], we chose pH 5 for all our measurements so that the carboxyl group in 2-AS is in its protonated state which is electrically neutral (see Fig. 1(c)) [32]. In addition, this also avoids any ground state heterogeneity due to ionization of the carboxyl group [32].

The fluorescence emission spectra for 2-AS in POPC and EPOPC vesicles are shown in Fig. 2. The emission maximum³ of 2-AS in POPC LUVs is found to be at 459 nm. However, in EPOPC vesicles the emission

³ We have used the term maximum of fluorescence emission in a somewhat wider sense here. In every case, we have monitored the wavelength corresponding to maximum fluorescence intensity, as well as the center of mass of the fluorescence emission. In most cases, both these methods yielded the same wavelength. In cases where minor discrepancies were found, the center of mass of emission has been reported as the fluorescence maximum.

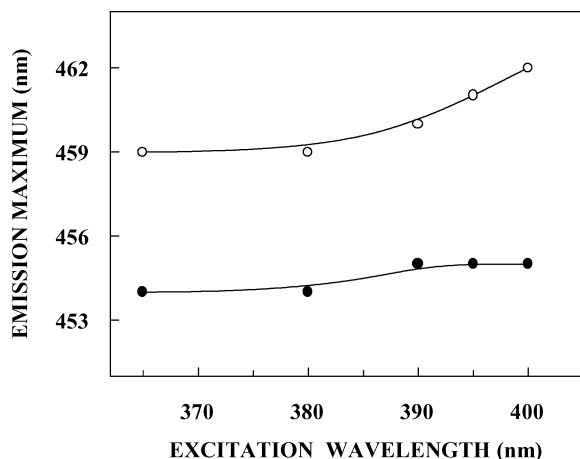


Fig. 3. Effect of changing excitation wavelength on the wavelength of maximum emission for 2-AS in LUVs of POPC (O) and EPOPC (●). All other conditions are as in Fig. 2. See Experimental for other details.

maximum displays a blue shift and is at 454 nm. This blue shift of the emission maximum indicates that there is a reduction in polarity in the region surrounding the anthroyloxy probe in EPOPC membranes. This could be due to decreased water content of EPOPC membranes compared to POPC membranes. In fact, it has previously been shown that the ethylphosphatidylcholine derivative for a series of saturated chain lipids has significantly reduced water content than the corresponding unesterified phosphatidylcholines in the fluid state [19,40].

The shifts in the maxima of fluorescence emission of 2-AS in POPC and EPOPC vesicles as a function of excitation wavelength are shown in Fig. 3. As the excitation wavelength is changed from 365 to 400 nm, the emission maximum of 2-AS in POPC vesicles shifts from 459 to 462 nm, which amounts to a REES of 3 nm. Such a shift in the wavelength of emission maximum with change in the excitation wavelength is characteristic of the red edge effect and indicates that the anthroyloxy moiety in 2-AS is localized in a motionally restricted region of the POPC membrane that offers considerable resistance to solvent reorientation in the excited state [16]. Interestingly, the emission maximum of 2-AS in EPOPC does not change significantly in this excitation range. The emission maximum of 2-AS in EPOPC vesicles shows a markedly reduced shift from 454 to 455 nm, *i.e.*, shows a REES of only 1 nm, as the excitation wavelength is changed from 365 to 400 nm. Thus, the magnitude of REES obtained for the same probe 2-AS varies with the overall charge of the host membrane. In other words, whereas 2-AS exhibits a REES of 3 nm in zwitterionic POPC membranes, it shows a minimal REES of 1 nm in the cationic EPOPC membrane. We attribute this to the change in the microenvironment

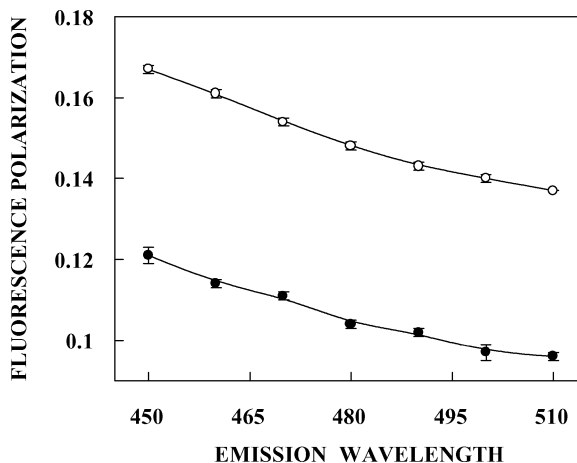


Fig. 4. Fluorescence polarization of 2-AS in POPC (O) and E-POPC (●) LUVs as a function of emission wavelength. The excitation wavelength was 365 nm in all cases. All other conditions are as in Fig. 2. The data points shown are the means \pm standard errors of at least four independent measurements. See Experimental for other details.

experienced by the probe in the two cases induced by the difference in charge of the two phospholipids.

Fig. 4 shows the variation in fluorescence polarization of 2-AS in POPC and EPOPC vesicles as a function of wavelength across the emission spectrum. The polarization of 2-AS in POPC and EPOPC vesicles shows a decrease with increasing emission wavelength with the lowest polarization being observed at the longest wavelength (red edge) where emission from the relaxed fluorophores predominates. Similar observations have previously been reported for other fluorophores in environments of restricted mobility [2]. More importantly, polarization values are found to be higher for 2-AS in POPC vesicles at all wavelengths than the corresponding values in EPOPC vesicles. This is indicative of the differential extent of rotational dynamics exhibited by 2-AS in these two types of vesicles. The higher polarization values for 2-AS in POPC vesicles imply that the environment of the probe is more restricted in POPC vesicles resulting in slower rotational diffusion when compared to 2-AS in EPOPC vesicles (assuming that the fluorescence lifetime of 2-AS in these two cases are similar; see later). This is consistent with the REES results reported above where we observed a higher REES for 2-AS in POPC vesicles implying a more restricted environment.

The above conclusion about the differential extent of rotational dynamics exhibited by 2-AS in POPC and EPOPC vesicles was rigorously tested by measuring fluorescence lifetimes of 2-AS in the two types of vesicles. A typical intensity decay profile with its biexponential fitting and the various statistical parameters used to check

Table I. Lifetimes of 2-AS in LUVs of Different Charge^a

Membrane type	α_1	τ_1 (ns)	α_2	τ_2 (ns)	$\langle \tau \rangle$ (ns)
Zwitterionic (POPC)	0.72	10.36	0.28	5.96	9.55
Cationic (EPOPC)	0.62	10.74	0.38	6.65	9.61

^aExcitation wavelength 365 nm; emission wavelength 460 nm.

the goodness of fit is shown in Fig. 5. Table I shows the fluorescence lifetimes of 2-AS in POPC and EPOPC vesicles. All fluorescence decays could be fitted well with a biexponential function. Table I shows that the mean lifetime, calculated using Eq. (3), of 1 mol% 2-AS in LUVs of POPC is 9.55 ns, whereas it is 9.61 ns in EPOPC vesicles. The similarity of these lifetime values implies that the apparent rotational correlation times calculated using the Perrin equation [29] would support our earlier conclusion, based on fluorescence polarization results (Fig. 4), about the differential extent of rotational dynamics exhibited by 2-AS in POPC and EPOPC vesicles.

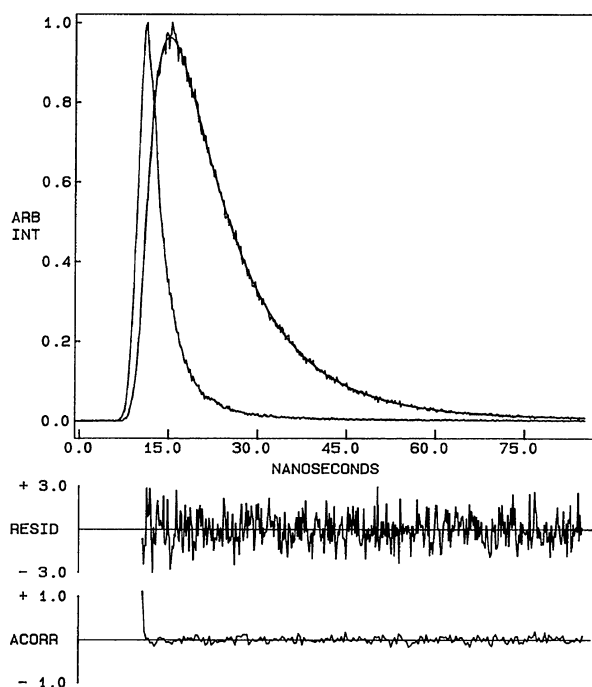


Fig. 5. Time-resolved fluorescence intensity decay of 2-AS in EPOPC LUVs. Excitation was at 365 nm and emission was monitored at 460 nm. The sharp peak on the left is the lamp profile. The relatively broad peak on the right is the decay profile, fitted to a biexponential function. The two lower plots show the weighted residuals and the autocorrelation function of the weighted residuals. The concentration of EPOPC was 0.85 mM and probe to lipid ratio was 1:100 (mol/mol). See Experimental for other details.

DISCUSSION

As mentioned above, the chemical structures of POPC and EPOPC are identical except that EPOPC has an ethyl group attached to one of the phosphate oxygen atoms through an ester bond. This neutralizes the negative charge resulting in the cationic nature of EPOPC due to the remaining positive charge on the choline headgroup. As a result of this difference in chemical structure, membranes formed by POPC and EPOPC would have different surface charge, and headgroup conformation and orientation (see later). Importantly, the interfacial regions of membranes formed by these phospholipids would also be different due to the difference in the headgroup charge and introduction of the hydrophobic ethyl group in case of EPOPC membranes.

Biological membranes are complex assemblies of lipids and proteins that allow cellular compartmentalization and act as the interface through which cells communicate with each other and with the external milieu. The communication between membranes and their aqueous surroundings is mediated by phospholipid headgroups and the membrane interfacial region. The phospholipid headgroup is generally oriented along the plane of the bilayer. However, this may not always be true in case of positively charged headgroups such as EPOPC. Previous NMR and neutron diffraction studies have shown that the lipid headgroups do not have a rigid orientation and are capable of changing their conformation in response to external stimuli such as pH and ionic gradient [41]. Interestingly, differential rates of solvent reorientation (relaxation) around excited state fluorophores have previously been reported for fluorophores embedded in membranes composed of phospholipids having different interfacial chemistry such as ester linked and ether linked phospholipids [42–44].

We report here that a small change in lipid chemistry resulting in a change in the membrane headgroup charge type and the interface can give rise to considerable difference in the microenvironment experienced by a membrane embedded molecule. Our results show that the microenvironment experienced by a membrane probe such as 2-AS is different in POPC and EPOPC membranes, as reported by the wavelength-selective fluorescence approach (specifically, REES), and other fluorescence parameters.

Previous results from our laboratory have shown that the wavelength-selective fluorescence is sensitive to depth-dependent solvent relaxation in membranes and thus can be used as a 'membrane dipstick' [16]. Furthermore, the wavelength-selective fluorescence approach can be used to probe the extent of water penetration in membranes [17], structural transition in micelles [45], and dynamics of hydration in reverse micelles [46]. The results presented here show that this approach can be used to detect differences in microenvironment induced by a change in membrane charge type.

An interesting feature of charged membrane surfaces is that it promotes the formation of a stable layer of hydration consisting of oriented water molecules which may stabilize the membrane headgroup and interfacial region [47]. The difference in environment encountered by the probe in the two cases may therefore be due to variation in hydration in the two membranes owing to different charges [19,40]. It is not clear whether this factor plays any role in the ability of cationic lipids such as EPOPC as transfection agents [30] and represents an interesting question.

ACKNOWLEDGMENTS

We thank Y.S.S.V. Prasad and G.G. Kingi for technical help. This work was supported by the Council of Scientific and Industrial Research, Government of India. D.A.K. thanks the University Grants Commission for the award of a Senior Research Fellowship. A.G. was awarded a Summer Training Program Fellowship by the Centre for Cellular and Molecular Biology. We sincerely acknowledge an initial gift of EPOPC from Robert C. MacDonald (Northwestern University, Evanston, Illinois). We thank members of our laboratory for critically reading the manuscript.

REFERENCES

1. A. Chattopadhyay and S. Mukherjee (1993). Fluorophore environments in membrane-bound probes: A red edge excitation shift study. *Biochemistry* **32**, 3804–3811.
2. S. Mukherjee and A. Chattopadhyay (1995). Wavelength-selective fluorescence as a novel tool to study organization and dynamics in complex biological systems. *J. Fluorescence* **5**, 237–246.
3. A. Chattopadhyay (2002). Application of the wavelength-selective fluorescence approach to monitor membrane organization and dynamics. In *Fluorescence Spectroscopy, Imaging and Probes*, R. Kraayenhof, A. J. W. G. Visser, and H. C. Gerritsen (Eds.), Springer-Verlag, Heidelberg, Germany, pp. 211–224.
4. A. Chattopadhyay (2003). Exploring membrane organization and dynamics by the wavelength-selective fluorescence approach. *Chem. Phys. Lipids* **122**, 3–17.
5. A. P. Demchenko (1988). Site-selective excitation: A new dimension in protein and membrane spectroscopy. *Trends Biochem. Sci.* **13**, 374–377.
6. A. P. Demchenko (2002). The red-edge effects: 30 years of exploration. *Luminescence* **17**, 19–42.
7. D. Haussinger (1996). The role of cellular hydration in the regulation of cell function. *Biochem. J.* **313**, 697–710.
8. P. Mentré (Ed.) (2001). Water in the cell. *Cell. Mol. Biol.* **47**, 709–970.
9. C. Ho and C. D. Stubbs (1992). Hydration at the membrane protein-lipid interface. *Biophys. J.* **63**, 897–902.
10. W. B. Fischer, S. Sonar, T. Marti, H. G. Khorana, and K. J. Rothschild (1994). Detection of a water molecule in the active-site of bacteriorhodopsin: Hydrogen bonding changes during the primary photoreaction. *Biochemistry* **33**, 12757–12762.
11. H. Kandori, Y. Yamazaki, J. Sasaki, R. Needleman, J. K. Lanyi, and A. Maeda (1995). Water-mediated proton transfer in proteins: An FTIR study of bacteriorhodopsin. *J. Am. Chem. Soc.* **117**, 2118–2119.
12. R. Sankaramakrishnan and M. S. P. Sansom (1995). Water-mediated conformational transitions in nicotinic receptor M2 helix bundles: A molecular dynamics study. *FEBS Lett.* **377**, 377–382.
13. S. Mukherjee and A. Chattopadhyay (1994). Motionally restricted tryptophan environments at the peptide-lipid interface of gramicidin channels. *Biochemistry* **33**, 5089–5097.
14. A. Chattopadhyay and R. Rukmini (1993). Restricted mobility of the sole tryptophan in membrane-bound melittin. *FEBS Lett.* **335**, 341–344.
15. A. K. Ghosh, R. Rukmini, and A. Chattopadhyay (1997). Modulation of tryptophan environment in membrane-bound melittin by negatively charged phospholipids: Implications in membrane organization and function. *Biochemistry* **36**, 14291–14305.
16. A. Chattopadhyay and S. Mukherjee (1999). Depth-dependent solvent relaxation in membranes: Wavelength-selective fluorescence as a membrane dipstick. *Langmuir* **15**, 2142–2148.
17. A. Chattopadhyay and S. Mukherjee (1999). Red edged excitation shift of a deeply embedded membrane probe: Implications in water penetration in the bilayer. *J. Phys. Chem. B* **103**, 8180–8185.
18. S. McLaughlin (1989). The electrostatic properties of membranes. *Annu. Rev. Biophys. Chem.* **18**, 113–136.
19. R. N. A. Lewis, I. Winter, M. Kriechbaum, K. Lohner and R. N. McElhaney (2001). Studies of the structure and organization of cationic lipid bilayer membranes: Calorimetric, spectroscopic, and X-ray diffraction studies of linear saturated P-O-Ethyl phosphatidylcholines. *Biophys. J.* **80**, 1329–1342.
20. J. C. Dittmer and R. L. Lester (1964). A simple, specific spray for the detection of phospholipids on thin-layer chromatograms. *J. Lipid Res.* **5**, 126–127.
21. C. W. F. McClare (1971). An accurate and convenient organic phosphorus assay. *Anal. Biochem.* **39**, 527–530.
22. R. P. Haugland (1996). *Handbook of Fluorescent Probes and Research Chemicals*, (6th Ed.), Molecular Probes Inc., Eugene, OR.
23. R. C. MacDonald, R. I. MacDonald, B. P. Menco, K. Takeshita, N. K. Subbarao, and L. R. Hu (1991). Small-volume extrusion apparatus for preparation of large, unilamellar vesicles. *Biochim. Biophys. Acta* **1061**, 297–303.
24. R. F. Chen and R. L. Bowman (1965). Fluorescence polarization: Measurement with ultraviolet-polarizing filters in a spectrophotofluorometer. *Science* **147**, 729–732.
25. P. R. Bevington (1969). *Data Reduction and Error Analysis for the Physical Sciences*, McGraw-Hill, New York.
26. D. V. O'Connor and D. Phillips (1984). *Time-Correlated Single Photon Counting*, Academic Press, London, 180–189.
27. R. A. Lampert, L. A. Chewter, D. Phillips, D. V. O'Connor, A. J. Roberts, and S. R. Meech (1983). Standards for nanosecond fluorescence decay time measurements. *Anal. Chem.* **55**, 68–73.
28. A. Grinvald and I. Z. Steinberg (1974). On the analysis of fluorescence decay kinetics by the method of least-squares. *Anal. Biochem.* **59**, 583–598.
29. J. R. Lakowicz (1999). *Principles of Fluorescence Spectroscopy*, Kluwer-Plenum Press, New York.

30. R. C. MacDonald, G. W. Ashley, M. M. Shida, V. A. Rakhmanova, Y. S. Tarahovsky, D. P. Pantazatos, M. T. Kennedy, E. V. Pozharski, K. A. Baker, R. D. Jones, H. S. Rosenzweig, K. L. Choi, R. Qiu, and T. J. McIntosh (1999). Physical and biological properties of cationic triesters of phosphatidylcholine. *Biophys. J.* **77**, 2612–2629.
31. A. T. Young, J. R. Lakey, A. G. Murray, and R. B. Moore (2002). Gene therapy: A lipofection approach for gene transfer into primary endothelial cells. *Cell Transplant* **11**, 573–582.
32. F. S. Abrams, A. Chattopadhyay, and E. London (1992). Determination of the location of fluorescent probes attached to fatty acids using parallax analysis of fluorescence quenching: Effect of carboxyl ionization state and environment on depth. *Biochemistry* **31**, 5322–5327.
33. K. R. Thulborn and W. H. Sawyer (1978). Properties and the locations of a set of fluorescent probes sensitive to the fluidity gradient of the lipid bilayer. *Biochim. Biophys. Acta* **511**, 125–140.
34. J. Villain and M. Prieto (1991). Location and interaction of *N*-(9-anthroyloxy)-stearic acid probes incorporated in phosphatidylcholine vesicles. *Chem. Phys. Lipids* **59**, 9–16.
35. R. Hutterer, F. W. Schneider, H. Lanig, and M. Hof (1997). Solvent relaxation behaviour of *n*-anthroyloxy fatty acids in PC-vesicles and paraffin oil: A time-resolved emission spectra study. *Biochim. Biophys. Acta* **1323**, 195–207.
36. A. Chattopadhyay and E. London (1987). Parallax method for direct measurement of membrane penetration depth utilizing fluorescence quenching by spin-labeled phospholipids. *Biochemistry* **26**, 39–45.
37. F. S. Abrams and E. London (1993). Extension of the parallax analysis of membrane penetration depth to the polar region of model membranes: Use of fluorescence quenching by a spin-label attached to the phospholipid polar headgroup. *Biochemistry* **32**, 10826–10831.
38. T. C. Werner and R. M. Hoffman (1973). Relation between an excited state geometry change and the solvent dependence of 9-methyl anthroate fluorescence. *J. Phys. Chem.* **77**, 1611–1615.
39. V. Von Tscharner and G. K. Radda (1981). The effect of fatty acids on the surface potential of phospholipid vesicles measured by condensed phase radioluminescence. *Biochim. Biophys. Acta* **643**, 435–448.
40. I. Winter, G. Pabst, M. Rappolt, and K. Lohner (2001). Refined structure of 1,2-diacyl-P-O-ethylphosphatidylcholine bilayer membranes. *Chem. Phys. Lipids* **112**, 137–150.
41. J. Seelig, P. M. Macdonald, and P. G. Scherer (1987). Phospholipid head groups as sensors of electric charge in membranes. *Biochemistry* **26**, 7535–7541.
42. J. B. Massey, H. S. She, and H. J. Pownall (1985). Interfacial properties of model membranes and plasma lipoproteins containing ether lipids. *Biochemistry* **24**, 6973–6978.
43. A. Sommer, F. Paltauf, and A. Hermetter (1990). Dipolar solvent relaxation on a nanosecond time scale in ether phospholipid membranes as determined by multifrequency phase and modulation fluorometry. *Biochemistry* **29**, 11134–11140.
44. L. A. Bagatolli, T. Parasassi, G. D. Fidelio, and E. Gratton (1999). A model for the interaction of 6-lauroyl-2-(*N,N*-dimethylamino)naphthalene with lipid environments: Implications for spectral properties. *Photochem. Photobiol.* **70**, 557–564.
45. S. S. Rawat and A. Chattopadhyay (1999). Structural transitions in the micellar assembly: A fluorescence study. *J. Fluorescence* **9**, 233–244.
46. A. Chattopadhyay, S. Mukherjee, and H. Raghuraman (2002). Reverse micellar organization and dynamics: A wavelength-selective fluorescence approach. *J. Phys. Chem. B* **106**, 13002–13009.
47. R. Kraayenhof, G. J. Sterk, H. W. Wong Fong Sang, K. Krab, and R. M. Epand (1996). Monovalent cations differentially affect membrane surface properties and membrane curvature, as revealed by fluorescent probes and dynamic light scattering. *Biochim. Biophys. Acta* **1282**, 293–302.